A cross saturation model for interior permanent magnet synchronous machine. Application to a starter-generator

L. Chédot*†
†Valeo Electrical System
2, rue A. Boulle / BP150
94017 Créteil Cedex / France
Email: laurent.chedot@utc.fr

G. Friedrich*
*University of Technology of Compiègne
Laboratory of Electromechanics / BP20529
60205 Compiègne Cedex / France
Email: guy.friedrich@utc.fr

***Abstract*— This paper deals with a cross saturation model for Interior Permanent Magnet Synchronous Machine (IPMSM) in starter-generator applications. After having shown the importance of the phenomenon of cross saturation for the constraining applications of the IPMSM, the authors propose a model based on the use of an off-line calculation by the finite element method whose results are integrated in dynamic simulation. A relatively reduced number (25) of off line FE simulations leads to a good precision in the taking into account of the dynamic phenomenon of cross saturation. The dynamic model suggested is then validated in steady operation and transient state within the framework of a starter-generator applications.**

I. INTRODUCTION

The Interior Permanent Magnet Synchronous Machine (IPMSM) is a challenger to the induction machine for starter generator applications [1]–[6]. Its main advantage is a high efficiency because of its low-losses rotor. Starter-generator applications requires a precise model in very constrained conditions. Flux weakening is needed and for cost reduction, the machine is highly saturated in the starter mode. The model needs a precise taking into account of the magnetic saturation [7], [8]. The starter generator is supplied by the mean of a PWM power converter: its influence has to be taken into account (pulsating torques due to the converter for example). From a simulation point of view, the electric machine is a component of a global system, so, the proposed model has to be sufficiently fast to be integrated in the global structure and avoiding prohibitive calculus times.

To this general constraints due to the application and common to all electric machines, IPMSM requires a precise modelisation of the cross saturation phenomenon. The phenomenon of cross saturation was studied for a certain number of years, but most of studies deal with the wound rotor synchronous machines. Since 1973, FUCHS, clearly highlighted the limitations of the model d, q in the case of high power wound rotor synchronous machine (WRSM - turboalternators) [9]. The same kind of study was realised on smooth [10] and salient pole WRSM [11], [12]. The authors showed the limitation of classical linear uncoupled model compared to experimental results. Moreover, some studies are integrally dedicated to the experimental validation of the saturation and the cross coupling [12]–[16].

The classical flux models taking into account of the cross saturation are based on the linear model. New flux representing the cross coupling of the other axes are added:

$$\psi_d = L_d(i_d, i_q)i_d + \psi_M + \psi_{dq}(i_d, i_q) \quad (1)$$
$$\psi_q = L_q(i_d, i_q)i_q + \psi_{qd}(i_d, i_q) \quad (2)$$

All flux are modeled by a constant [17] or a variable inductance [12]. The inductances can be used directly and modeled by an unlinear function [18]–[23], or expressed as the product of an unsaturated inductance ($L_{d\ uns}$) and a saturation coefficient depending on currents [13]: $\psi_d(i_d, i_q) = L_d i_d$ with $L_d = f(i_d, i_q)$ or $L_d = L_{d\ uns}S_d(i_d, i_q)$ (and the same for the q axe). We can find lots of applications based on this approach [24]–[27].

The previous models are used to predict steady-state behaviour and performances. Other models were developed in order to evaluate the dynamic response of these machines. VAS gives a complete synthesis of dynamic approaches [28]. Classically, these models are expressed as equivalent electric circuit taking into account of each inductance derivative (see [29], [30] as examples). The references concerning this kind of model dealt with constant speed WRSM and studied perturbations on the network. Recent studies about dynamic models are less common but we can find some complete studies [31], [32].

It was shown that the cross saturation phenomenon was studied on WRSM. The models and the identification procedures were especially developed for this kind of machine. On the contrary, only a few studies and models dedicated to the IPMSM can be found. Classical experimental testing are not appropriate to constant field, due to permanent magnet, synchronous machines. Thus the study of the cross saturation with this type of machine with dynamic performances becomes of the greatest importance. The presented modelisation proposes a fast dynamic model using off line Finite Elements (FE) calculus. This model fulfils with presented constraints and simulations will be compared to experimental results for flux weakening (high speed generator mode).

II. MODEL DESCRIPTION

A. Linear model

Although linear hypothesis are inadequate in our application, a reminder may be useful to precise our modelling. Generally, dynamic analysis of electric machine are made in the d,q frame (Park transform). In this formulation, no hypothesis has to be made on the voltage supply waveforms. Sinusoidal waveforms are a particular case of the supply but are not required by the modelisation. Only the MMF waveform have to be considered sinusoidal [33], [34].

On the other hand, the Park transform is a purely geometric transformation and so, is not linked to linear hypothesis. Equations 3, 4, and 5 stay true whatever magnetic saturation and voltage waveforms are.

In such hypothesis, the equations of the IPMSM are reduced to:

- Voltage equations

$$v_d = R_s i_d + \frac{d\psi_d}{dt} - w_s \psi_q \quad (3)$$

$$v_q = R_s i_q + \frac{d\psi_q}{dt} + w_s \psi_d \quad (4)$$

- Torque equation

$$T_{em} = p(\psi_d i_q - \psi_q i_d) \quad (5)$$

Flux are also deduced:

$$\psi_d = \int (v_d - R_s i_d + \omega_s \psi_q) \quad (6)$$

$$\psi_q = \int (v_q - R_s i_q - \omega_s \psi_d) \quad (7)$$

In the linear case, currents are quickly deduced from flux:

$$i_d = \frac{\psi_d - \psi_M}{L_d} \quad (8)$$

$$i_q = \frac{\psi_q}{L_q} \quad (9)$$

The voltage equations may be expressed by structural diagrams as on figure 1:

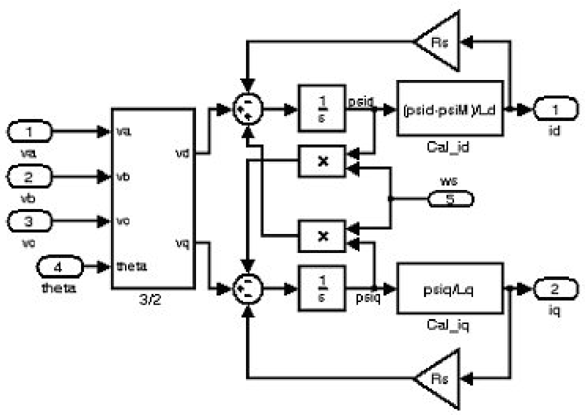

Fig. 1. Structural diagram of a linear IPMSM

This structural diagram, directly used in dynamic simulations like Matlab-Simulink [35], give instantaneous current for any input voltages. Currents and flux are the inputs for the calculation of electromagnetic flux. This result is only true for a linear behaviour.

B. Taking into account of the magnetic saturation

As seen on figure 1, the unique source of non linearity is the link between the flux and the currents. Of course, the notion of constant inductances is impossible to apply with saturated machines. Beyond that, IPMSM has a high coupling level between the two axis, so the determination of ψ_d requires to compute the contribution of i_d but also of i_q. The coupling between d and q axes is unavoidable. Nevertheless, projection of space vectors on a d-q frame linked to the rotor remain possible (purely geometric transformation) [16].

The proposed solution may be exposed in two parts:

- Determination of ψ_d and ψ_q as a function of i_d and i_q by an off line FE method (FLUX 2D)

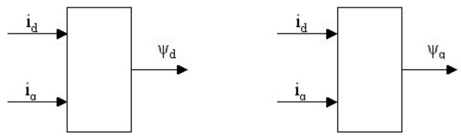

Fig. 2. Flux models

- inversion of the proposed model. As previously exposed on figure 1, dynamic model needs the knowledge of ψ_d and ψ_q, and therefore an inversion of the previous flux model. Like we will see later, the determination of the flux models (figure 2) needs different computations corresponding to different couple of $i_d,\ i_q$. In our case, we choose five values of i_d and i_q (25 FE computations) so, the numeric inversion needs an interpolation.

C. Determination of $\psi_d,\ \psi_q$ as a function of $i_d,\ i_q$

We can find the detail of this section in [7]. For different operating points (i_d, i_q), and in presence of the permanent magnets, the 3 phase flux (ψ_a, ψ_b, ψ_c) are evaluated and so, direct and quadrature flux are deduced:

$$\begin{pmatrix} i_d \\ i_q \end{pmatrix} \rightarrow Park^{-1} \rightarrow \begin{pmatrix} i_a \\ i_b \\ i_c \end{pmatrix} \rightarrow$$

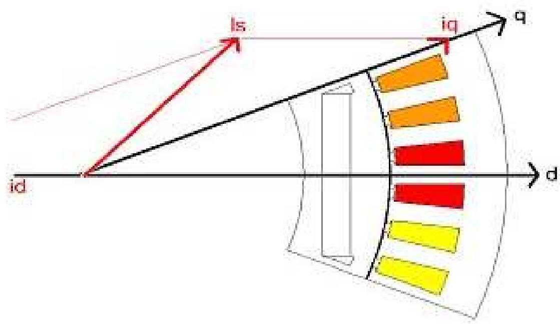

Fig. 3. Currents (area and vector) in a machine pole

which give after resolution:

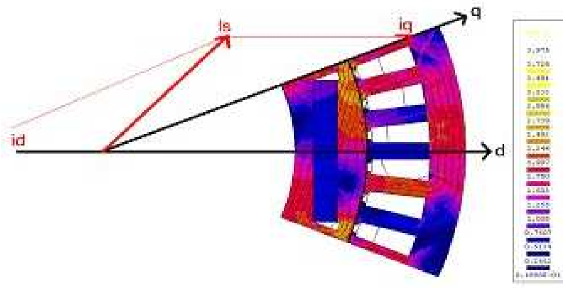

Fig. 4. Flux density and equiflux in a machine pole

$$\rightarrow \begin{pmatrix}\psi_a\\ \psi_b\\ \psi_c\end{pmatrix} \rightarrow \quad Park \quad \rightarrow \begin{pmatrix}\psi_d\\ \psi_q\end{pmatrix}$$

To evaluate the 3 phase flux (ψ_a, ψ_b, ψ_c), we use the classical method (see figure 5) [36]:

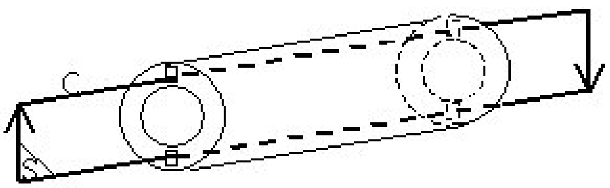

Fig. 5. Vector potential trajectory

Stockes theorem is applied to vector potential A.

$$\oint_C \vec{A}.\vec{dl} = \int\int_S \overrightarrow{rot}(\vec{A})dS \tag{10}$$

A is null outside the machine, so equation 10 became:

$$L_Z(A_+ - A_-) = \int\int_S \vec{B}dS = \Phi \tag{11}$$

Or, it is easy to evaluate the average potential in a yoke thanks to finite element software. This method is used for the three phases.

Figures 6 and 7 show ψ_d and ψ_q in function of i_d and i_q. Figure 7 shows a classic saturation curve for ψ_q as

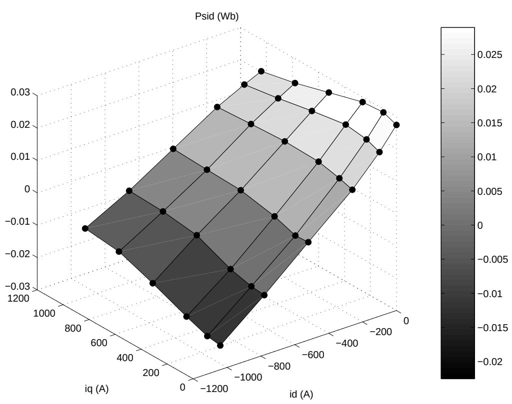

Fig. 6. flux ψ_d function of currents i_d, i_q

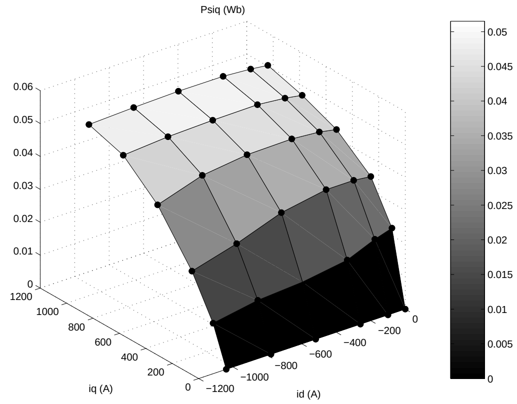

Fig. 7. flux ψ_q function of currents i_d, i_q

a function of i_q. It is important to notice a relatively low coupling between i_d and ψ_q. Nevertheless, figure 6 shows a high coupling between ψ_d and i_q, especially for negative high values of i_d. The taking into account of the cross saturation phenomenon is therefore fundamental for the modelling of high performance IPMSM.

D. Inversion of the flux model

1) Cross saturation neglected: if cross saturation is neglected, ψ_d is only linked to i_d (no i_q influence). As previously developed, with the use of FE methods, determination of ψ_d under saturation hypothesis is easy as long as i_d and the machine geometry are known. As shown on figure 8, our model needs $i_d = f(\psi_d)$ dynamic transfert function, thus, an inversion of the flux model.

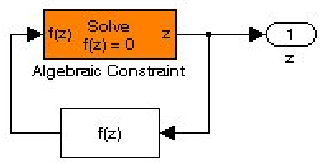

Fig. 8. Algebraic constraint bloc

The inversion of the flux model is based on a numerical tool (algebraic constraint) which computes its output to cancel its input. We can apply this function to inverse our flux model. As shown on figure 9, previous FE results have been tabulated.

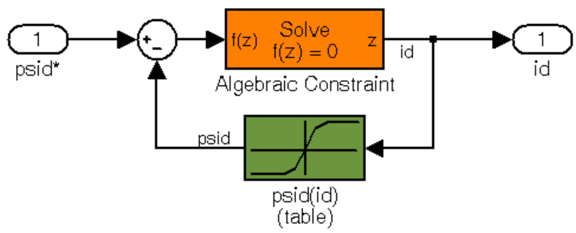

Fig. 9. Flux ψ_d computation

The *algebraic constraint* function computes i_d to cancel its input constituted by the difference between ψ_d^* and ψ_d. So, our flux model has been inverted.

2) Taking into account of the cross saturation: the same technique can be used for taking into account of the coupling between d and q axis. ψ_d and ψ_q computing are based on a 2D table instead of a 1D table when cross saturation is neglected.

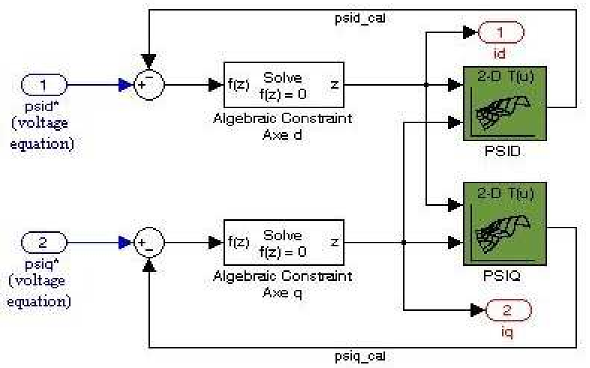

Fig. 10. Flux inversion (saturation and coupling included)

III. Steady state model validation

The detail of optimal control laws calculation can be found in [7]. Experience, and also simulation, are realised in the following conditions:

- for optimal control laws calculation, temperature is close to the ambient temperature ($T = 25^oC$), stator resistance is therefore equal to: $R_s = 6.1\ m\Omega$;
- current is limited by inverter: $I_{lim} = 200\ \hat{A}$;
- in motor mode, voltage is limited by the DC supply (40 V). In generator mode, the DC voltage is regulated by an active load to 42 V.

Figure 11(a) shows efficiencies measured in the torque vs. speed plan. Theoretical results are shown in comparison. It can be seen that the operating range is rather respected. Inside this operating range, measurements are very closed to the simulations. Globally, the efficiencies are low at low speed or low torque. They tend to 0.85 when power increases.

Figures 11(b) and 11(c) show efficiencies and electric power measured in the torque vs. speed plan. Theoretical results are shown in comparison. As in motor mode, we show that the operating range is the same in the simulation and in the real experimentation. Efficiencies reach to 0.91 and the electric power to $6300\ W$.

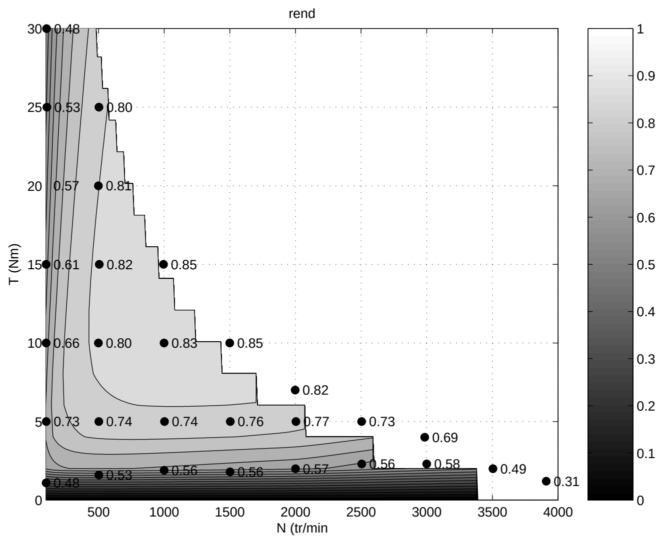

(a) Motor mode: efficiencies

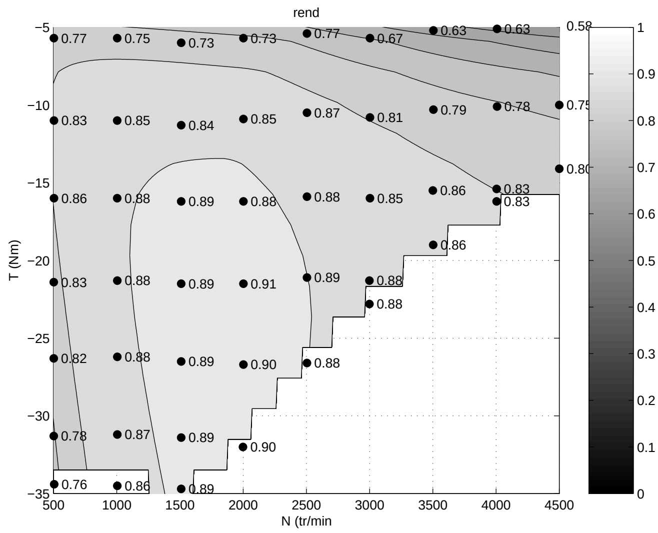

(b) Generator mode: efficiencies

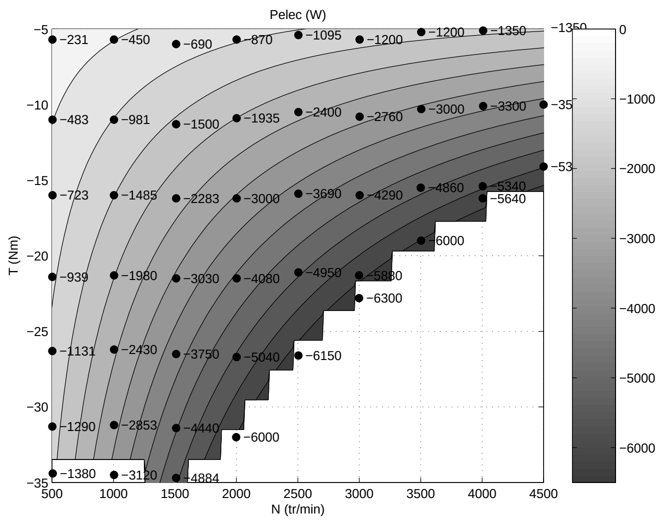

(c) Generator mode: electric power

Fig. 11. Steady-state results (isolines: simulation, points : measurements)

IV. Dynamic model validation

The simulation takes into account all real components:

- Machine: saturation and losses;
- Inverter: SPWM;
- DC load: active load (Ral-Lal-Cal + PWM) and DC bus (Lp-Cd);
- Speed is constant;
- Control: the machine is controlled by the optimal control laws, torque reference consists in a step from -5 Nm to -20 Nm (generator).

The detail of each part can be found in [7].

Figures 12, 13 and 14 show the evolution of torques, d and q currents (reference, simulation and measurements).

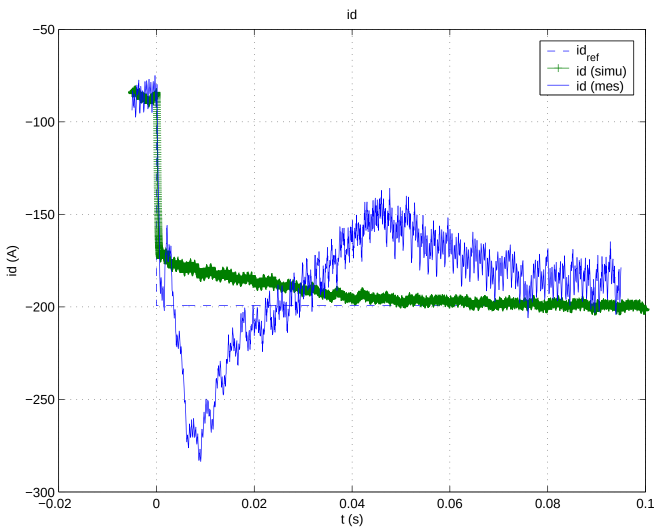

Fig. 12. Direct current in torque step test

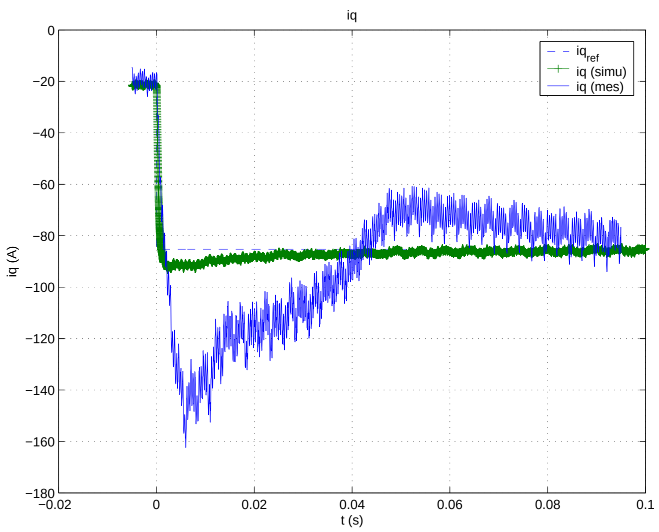

Fig. 13. Quadrature current in torque step test

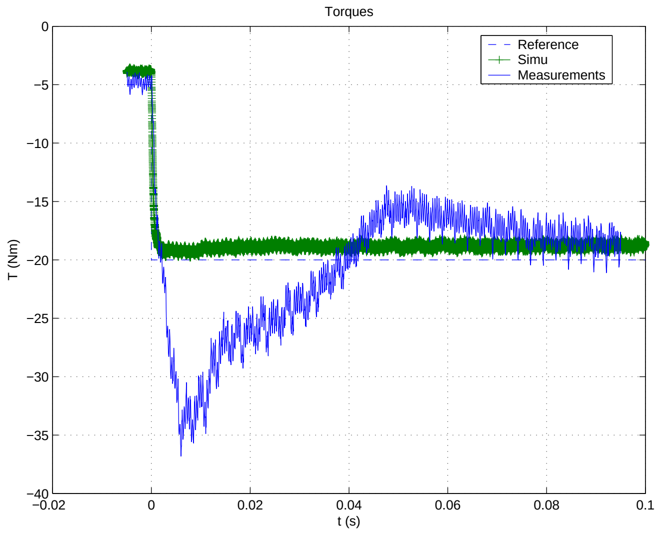

Fig. 14. Torques in torque step test

Observations:

- at 3000 rpm, the main current is the d-axis current in order to obtain the optimal flux-weakening;
- current regulators are efficient, d and q currents follow strictly and quickly the current reference from the optimal control tables. The inverter saturates a little when the step occurs, but currents control is never lost;
- we can detect a little overshoot in measured currents. The decoupling is not as efficient as in simulation but stay quite good. The dynamic model is therefore validated;
- the torque step response takes 100 ms. During this time, electric power rises from 1000 W to 6000 W. It means that the machine is able to deliver its maximum electric power in about 100 ms.

V. Test bench description

All the test are realised on a specific test bench (LEC) especially adapted to ISG (and SG).

Figure 15 shows the detail of the inverter. It is developed by the LEC, and is at present limited to 200 A for a 10 kHz chopping frequency. A 600 A version is under tests.

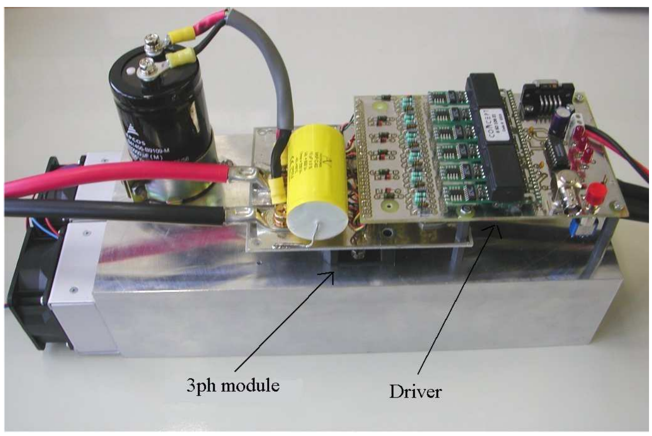

Fig. 15. Inverter (LEC)

Figure 16 gives a machine zoom. The integrated topology is immediately pointed out.

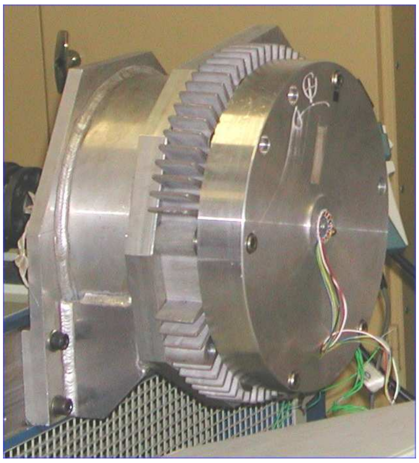

Fig. 16. ISG (Valeo-LEC)

All the controls (including PWM) and acquisitions (rotor position, phases currents, temperature, ad.) are done by a DSpace card (DS1103). All internal and external variables can be displayed and recorded.

VI. CONCLUSION

After having shown the importance of the cross saturation phenomenon for the constraining applications of the IPMSM, the authors proposed a model based on the use of an off-line calculation by the finite element method which results were integrated in dynamic simulation. A relatively reduced number (25) of off line FE simulations lead to a good precision in the taking into account of the dynamic phenomenon of cross saturation. The dynamic model suggested was then validated in steady operation and transient state within the framework of a starter-generator application.

A special design of the permanent magnet synchronous machine allows high flux weakening operation associated to high efficiencies (80 % in the flux weakening zone and up to 90 % at the limit of the constant torque zone). Dynamic performances are of excellent quality (less than 100 ms for a 5 kW step power requirement).

The proposed study has shown that IPMSM is a good challenger to the induction machine for high performance ISG or even for parallel hybrid vehicles applications.

REFERENCES

[1] B. CHALMERS, L. MUSABA, and D. GOSDEN, "Variable-frequency synchronous motor drives for electrical vehicles," *IEEE Trans. Ind. Appl.*, vol. 32, no. 4, pp. 896–903, Jul./Aug. 1996.

[2] E. LOVELACE, T. JAHNS, J. KIRTLEY, and J. LANG, "An interior PM starter-alternator for automotive applications," in *Int. Conf. Electrical machines*, Istanbul, Sep. 1998, pp. 1802–1808.

[3] J. HADJI-MINAGLOU and G. HENNEBERGER, "Comparison of different motor types for electric vehicle application," *EPE Journal*, vol. 8, no. 3-4, pp. 46–55, Sep. 1999.

[4] G. FRIEDRICH, L. CHÉDOT, and J. BIEDINGER, "Comparison of two optimal machine design for integrated starter-generator applications," in *Int. Conf. Electrical machines*, Aug. 2002.

[5] C. PLASSE, M. CHEMIN, G. LACAMOIRE, and E. VON WESTERHOLT, "L'alterno-démarreur, du stop & go au groupe motopropulseur hybride," in *Congrès de la Société des Ingénieurs Automobile*, Versaille, Nov. 2001.

[6] C. PLASSE, A. AKEMAKOU, P. ARMIROLI, and D. SEBILLE, "L'alterno-démarreur, du stop & go au groupe motopropulseur mild hybride," in *Prop'Elec*, Aix-en-Provence, Mar. 2003.

[7] L. CHÉDOT and G. FRIEDRICH, "Comparison of direct and adaptative optimal controls for interior permanent magnet synchronous integrated starter-generator," in *Int. Elec. Mach. Drive Conf.*, Madison, WI, Jun. 2003.

[8] ——, "Optimal control of interior permanent magnet synchronous integrated starter-generator," in *Conf. European Power Electronics Ass.*, Toulouse, Sep. 2003.

[9] E. FUCHS and E. ERDELYI, "Nonlinear theory of turboalternators, part II. Load dependent synchronous reactances," *IEEE Trans. Power App. Syst.*, vol. 92, no. 2, pp. 592–599, Apr. 1973.

[10] P. VAS, K. HALLENIUS, and J. BROWN, "Cross-saturation in smooth-air-gap electrical machines," *IEEE Trans. Energy Conv.*, vol. 1, no. 1, pp. 103–112, 1986.

[11] M. KAMOUN and M. POLOUJADOFF, "Experimental study of the effect of saturation on the steady state operation of a salient pole microalternator," *Elec. Mach. Power Syst.*, vol. 10, pp. 325–334, 1985.

[12] E. RICHTER and T. NEUMANN, "Saturation effects in salient pole synchronous motors with permanent magnet excitation," in *Int. Conf. Electrical machines*, vol. 2, Sept. 1984, pp. 603–606.

[13] A. EL-SERAFI, A. ABDALLAH, M. EL-SHERBINY, and E. BADAWY, "Experimental study of the saturation and the cross-magnetizing phenomenon in saturated synchronous machines," *IEEE Trans. Energy Conv.*, vol. 3, no. 4, pp. 815–823, Dec. 1988.

[14] B. CHALMERS, "Influence of saturation in brushless permanent-magnet motor drives," *IEE, part B*, vol. 139, pp. 51–52, 1992.

[15] W. SOONG and T. MILLER, "Practical field-weakening performance of the five classes of brushless synchronous AC motor drive," in *Conf. European Power Electronics Ass.*, 1993, pp. 303–310.

[16] B. STUMBERGER, G. STUMBERGER, D. DOLINAR, A. HAMLER, and M. TRLEP, "Evaluation of saturation and cross-magnetization effects in interior permanent-magnet synchronous motor," *IEEE Trans. Ind. Appl.*, vol. 39, no. 5, pp. 1264–1271, Sep./Oct. 2003.

[17] B. SNEYERS, D. NOVOTNY, and T. LIPO, "Field weakening in buried permanent magnet AC motor drives," *IEEE Trans. Ind. Appl.*, vol. 21, pp. 398–407, Mar./Apr. 1985.

[18] F. PARASILITI and P. POFFET, "A model for saturation effects in high-field permanent magnet synchronous motors," *IEEE Trans. Energy Conv.*, vol. 4, no. 3, pp. 487–494, Sep. 1989.

[19] L. XU, X. XU, T. LIPO, and D. NOVOTNY, "Vector control of a synchronous reluctance motor including saturation and iron loss," *IEEE Trans. Ind. Appl.*, vol. 27, pp. 977–985, 1991.

[20] M. ARJONA LOPEZ and D. MACDONALD, "A new lumped steady-state synchronous machine model derived from finite element analysis," *IEEE Trans. Energy Conv.*, vol. 14, no. 1, pp. 1–7, Mar. 1999.

[21] K. IDE, S. WAKUI, K. SHIMA, and M. TAKAHASHI, "Analysis of saturated synchronous reactances of a large turbine generator by considering cross-magnetizing reactances using finite elements," *IEEE Trans. Energy Conv.*, vol. 14, no. 1, pp. 66–71, Mar. 1999.

[22] E. LEVI, "Saturation modelling in d-q axis models of salient pole synchronous machine," *IEEE Trans. Energy Conv.*, vol. 14, no. 1, p. 44, Mar 1999.

[23] E. LOVELACE, T. JAHNS, and J. LANG, "Impact of saturation and inverter cost on interior PM synchronous machine drive optimization," *IEEE Trans. Ind. Appl.*, vol. 36, no. 3, pp. 681–689, May./Jun. 2000.

[24] A. EL-SERAFI, J. WU, and A. ABDALLAH, "Saturation representation in synchronous machine models," *Elec. Mach. Power Syst.*, vol. 20, pp. 355–369, 1992.

[25] A. EL-SERAFI and A. ABDALLAH, "Saturated synchronous reactances in synchronous machines," *IEEE Trans. Energy Conv.*, vol. 7, no. 3, pp. 355–369, Sep. 1992.

[26] A. EL-SERAFI and J. WU, "Determination of the parameters representing the cross-magnetizing effect in saturated synchronous machines," *IEEE Trans. Energy Conv.*, vol. 8, no. 3, pp. 333–342, Sep. 1993.

[27] F. MENU, "Modélisation de la machine synchrone à rotor bobiné et à pôles saillants dans les applications véhicules électriques," Rapport de DEA, Université de Technologie de Compiègne, Laboratoire d'Electromécanique de Compiègne, 1996.

[28] P. VAS, *Vector control of AC machines*. Springer, 1990.

[29] I. BOLDEA and S. NASAR, “A general equivalent circuit (GEC) of electric machines including crosscoupling saturation and frequency effects,” *IEEE Energy Conv.*, vol. 3, no. 3, pp. 689–695, Sep. 1988.

[30] J. OJO and T. LIPO, “An improved model for saturated salient pole synchronous motors,” *IEEE Trans. Energy Conv.*, vol. 4, no. 1, pp. 135–142, Mar. 1989.

[31] S.-A. TAHAN and I. KAMWA, “A two-factor saturation model for synchronous machines with multiple rotor circuits,” *IEEE Trans. Energy Conv.*, vol. 10, no. 4, pp. 609–616, Dec. 1995.

[32] C. MADEMLIS and V. AGELIDIS, “On considering magnetic saturation with maximum torque per current control in interior permanent magnet synchronous motor drives,” *IEEE Trans. Energy Conv.*, vol. 16, no. 3, pp. 246–252, Sep. 2001.

[33] G. SÉGUIER and F. NOTELET, *Electrotechnique industrielle*. Technique et documentation, 1994.

[34] J. LESENNE, G. SÉGUIER, and F. NOTELET, *Introduction à l’électrotechnique appronfondie*. Technique et documentation, 1980.

[35] *Matlab user’s guide*, The MathWorks Inc., 2000.

[36] N. IDA and J. BASTOS, *Electromagnetics and calculation of fields*. Springer, 1997.